

Evidence for nonmonotonic magnetic field penetration in a type-I superconductor

V.F. Kozhevnikov^{1*}, C.V. Giuraniuc¹, M.J. Van Bael¹, K. Temst², C. Van Haesendonck¹,
T.M. Mishonov³, T. Charlton⁴, R.M. Dalglish⁴, Yu.N. Khaidukov⁵, Yu.V. Nikitenko⁵,
V.L. Aksenov⁵, V.N. Gladilin^{1,6}, V.M. Fomin⁶, J.T. Devreese⁶, and J.O. Indekeu¹

¹Laboratorium voor Vaste-Stoffysica en Magnetisme Katholieke Universiteit Leuven, 3001 Leuven, Belgium

²Instituut voor Kern- en Stralingsfysica, Katholieke Universiteit Leuven, 3001 Leuven, Belgium

³Department of Theoretical Physics, St Clement of Ohrid University of Sofia, 1164 Sofia, Bulgaria

⁴ISIS Science Division, Rutherford Appleton Laboratory, Chilton, Didcot OX11 0QX, United Kingdom

⁵Frank Laboratory of Neutron Physics, Joint Institute for Nuclear Research, 141980 Dubna, Moscow Region, Russia

⁶Theoretische Fysica van de Vaste Stoffen, Universiteit Antwerpen, 2020 Antwerpen, Belgium

(Dated: February 8, 2022)

Polarized neutron reflectometry (PNR) provides evidence that *nonlocal* electrodynamics governs the magnetic field penetration in an extreme low- κ superconductor. The sample is an indium film with a large elastic mean free path (11 μm) deposited on a silicon oxide wafer. It is shown that PNR can resolve the difference between the reflected neutron spin asymmetries predicted by the local and nonlocal theories of superconductivity. The experimental data support the nonlocal theory, which predicts a *nonmonotonic decay* of the magnetic field.

PACS numbers: 74.20.-z, 74.25.Ha, 78.70.Nx

In this paper we pose and answer experimentally the following fundamental questions. Are nonlocal electrodynamics effects measurable in superconductors? Can the nonmonotonic decay of magnetic field penetration predicted by the nonlocal theory be observed? To what extent can Polarized Neutron Reflectometry (PNR) resolve the difference between local and nonlocal diamagnetic responses expected for strongly type-I superconductors?

Nonlocality is a key concept of superconductivity theory, but its experimental verification is still not established. In the Meissner state, a magnetic field applied parallel to the surface located at $z = 0$ causes the magnetic induction $B(z)$ to penetrate over a depth $\lambda \equiv B(0)^{-1} \int B(z) dz$. In the London (*local*) limit, appropriate to most type-II superconductors, $B(z) \propto \exp(-z/\lambda_L)$, where λ_L is the London penetration depth. In 1953, to explain the variation of λ in type-I superconductor Sn caused by adding In, Pippard proposed that the current density is related to the average of the vector potential over a region of size ξ_0 (the Pippard coherence length) [1]. The smaller the Ginzburg-Landau parameter κ , the more important this *nonlocal* effect.

Nonlocal theory predicts that $B(z)$ deviates from a simple exponential decay. $B(z)$ is *nonmonotonic* and, moreover, *changes sign* at a specific depth [1]. In the pure limit ($\xi_0 \ll \ell$, where ℓ is the elastic mean free path) $B(z)$ is determined by the intrinsic parameters $\lambda_L(T = 0)$ and ξ_0 , and by the temperature T . The deviation is most significant in “extreme” type-I superconductors ($\kappa \ll 1/\sqrt{2}$), such as Al ($\kappa \approx 0.01$) and In (0.06). For these the results of the Pippard theory are identical to those of the Bardeen-Cooper-Schrieffer theory [2]. On the other hand, the local approximation is safe for $\kappa > 1.5$ [3], i.e., marginal nonlocal effects are predicted for some type-II superconductors such as Nb ($\kappa \approx 1$).

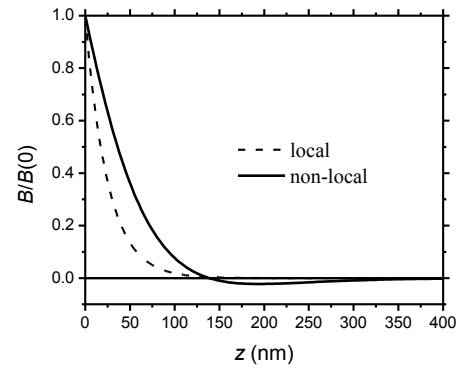


FIG. 1: Magnetic-induction profiles $B(z)$ in a semi-infinite In sample. The dashed (solid) line corresponds to the local (non-local) relation between current density and vector potential.

$B(z)$ in In, calculated in local and nonlocal approaches, in the pure limit with $\xi_0 = 0.38 \mu\text{m}$ and $\lambda_L(0) = 0.025 \mu\text{m}$ [4], for $T = 1.8 \text{ K}$, is shown in Fig. 1. Details about the formalism can be found in Ref. 3. In the nonlocal approach $B(2\lambda_L)/B(0) \approx 1/e$. The sign reversal is expected at $z \approx 5.5 \lambda_L$, and the amplitude of the reversed field is at most about 3% of the field at the surface.

An observation of sign reversal was reported in Ref. 5. An external AC magnetic field H with amplitude up to 30 Oe was applied parallel to a hollow cylindrical Sn film about 2 μm thick, and a strongly attenuated (10^8 times) signal with reversed phase was detected inside the cylinder at $T = 2.88 \text{ K}$ and $H \approx 25 \text{ Oe}$. This phase difference was interpreted as a change of sign in the penetrating field. However, this is questionable because the phase difference drops back to zero at a larger (30 Oe) field, whereas the critical field H_c at 2.9 K is 115 Oe [6].

Nowadays $B(z)$ can be measured directly using polarized neutron reflectometry (PNR) [7] and low-energy muon spin rotation (LE- μ SR) [8] techniques. We comment briefly on the latter before focusing on the former.

In the LE- μ SR technique positive muons polarized perpendicularly to the applied field are implanted in a sample over a distance determined by the muon energy. $B(z)$ is obtained from measuring the Larmor precession frequency of the muon spins at stopping distance. In other words, the implanted muons serve as tiny sensors of the magnetic field inside the sample. However, in practice the muon precession is progressively damped with depth due to a broad distribution of stopping distances [9]. From our prospectus, this is the main difficulty in applying the LE- μ SR technique to fields with a sharp profile.

Recently, the LE- μ SR technique was used to measure $B(z)$ in Pb, Nb, and Ta [9]. Most interesting is the observation of a non-exponential shape of $B(z)$ for all studied metals. The nonlinearity of the semi-log plots for $B(z)$ is marginal, which is exactly what should be expected theoretically in view of the fairly high κ of the studied samples. For example, κ of pure Nb (residual resistivity ratio $RRR = 1600$) is 1.3 at 3 K and 1.0 at 7 K [10]. However, in Ref. 9 κ of less pure Nb ($RRR=133$) is reported to be 0.7 at 2.96 K and 7.6 K. This and some other inconsistencies with well established literature data suggest that the muon probing results may contain some hidden uncertainties. Therefore, additional experiments would be worthwhile, in particular on low- κ superconductors.

The PNR technique is based on the change of the neutron index of refraction in a magnetized medium. When a collimated neutron beam polarized along the magnetic field is incident on a flat, laterally uniform sample under a grazing angle, its specular reflectivity R is determined by the profile of the neutron scattering potential below the surface. R is measured versus momentum transfer $Q = 4\pi \sin \theta / \lambda_n$, where θ is the angle of incidence and λ_n the neutron wavelength. The scattering potential consists of a nuclear and a magnetic part, which results in different reflectivities R^+ and R^- for neutrons with spins polarized parallel (up) and anti-parallel (down) to the applied field, respectively. Direct information about the sample magnetization is obtained by combining R^+ and R^- ; the combination $s = (R^+ - R^-)/(R^+ + R^-)$ is the spin asymmetry. $B(z)$ can be found by fitting $s(Q)$ data with $s(Q)$ calculations based on theoretical models for $B(z)$. PNR has been applied for measuring the penetration depth and for detecting surface superconductivity in Nb [11, 12], high- T_c cuprates [13, 14, 15] and Pb [16, 17].

The nonlocal effect in $B(z)$ measured with PNR was discussed in Refs. 11, 12, 16 and 17. Although some deviation from exponential decay was noticed in Refs. 12 and 16, no solid confirmation of the nonlocal theory was obtained. The authors of Ref. 17 correctly pointed out that experiments with low- κ type-I superconductors are desirable to verify nonlocality, but their overall conclusion was that PNR is incapable of detecting nonlocality in *any* superconductor. In this light it is very interesting to

reassess the problem of nonlocality with state-of-the-art PNR applied to a low- κ material such as In, since during the last decade many neutron source facilities have significantly progressed in neutron flux, neutron optics and detector technology.

The design of the sample for the PNR study is based on the following requirements. The irradiated surface must be flat and possess minimal possible roughness. The sample must be thick enough to have the same electromagnetic properties as the bulk material. Degradation of the surface quality with increasing thickness limits the film thickness. Neutrons reflected back from the substrate should have a negligible effect on the reflectivity in a region close to the critical edge of total reflection, Q_c , where the reflectivity is most sensitive to the magnetic properties.

Two approaches can meet these requirements. One is to deposit a thick film on a flat substrate that reflects least. This can be achieved if the neutron refraction index of the substrate is larger than that of the sample. This approach was taken in the experiments on Nb [11, 12] and Pb [16, 17]. In fact, this was the only option, in view of the negligibly small absorption of neutrons in Nb and Pb. However, In is a strong absorber, which enables one to rely on substrates with a refractive index smaller than that of In, provided the thickness of the indium film is properly optimized. In this approach a second plateau or “hill”, associated with total reflection from the sample-substrate interface, is expected in the reflectivity curve $R(Q)$. This should yield additional information about the sample structure. Modelling shows that an indium thickness of 2.5 μm is appropriate. Such a sample was fabricated in the present work.

High purity indium (99.9999%) was deposited by thermal evaporation on the polished side of a silicon oxide wafer at room temperature. The substrate size was $2 \times 2 \text{ cm}^2 \times 1 \text{ mm}$. The base pressure and the evaporation rate were 4×10^{-8} mbar and 60-70 $\text{\AA}/\text{s}$, respectively. The nominal film thickness, as recorded by a quartz monitor, was 2.5 μm . Several smaller area samples were simultaneously fabricated for the film characterization.

The root-mean-square (rms) surface roughness σ probed with an atomic force microscope (AFM) yielded 2.0, 6.7 and 8.0 nm at the scale of 1, 5 and 10 μm , respectively. A scan range up to 10 μm was not sufficient to reach saturation of the roughness. Consequently, 8.0 nm is a lower bound on the roughness at the scale of the neutron coherence length ($\approx 100 \mu\text{m}$ [18]). In our simulations, effects due to surface roughness are modelled using Névot-Croce factors [7], where the roughness is characterized by σ ; it was allowed to vary to fit the experimental data.

Another parameter associated with the sample surface is the thickness of the indium oxide film. When exposed to air, In, like its neighbors in the Periodic Table, Al and Ga, instantly forms a protective oxide layer. A surface of indium in air remains lustrous for years. This suggests that the oxide layer is very thin, perhaps of the order

of a few monolayers, and should not affect the neutron reflectivity. This is consistent with the negative result of Rutherford backscattering measurements performed on our sample: no oxide film has been detected.

The electromagnetic properties of the sample were characterized by measurements of the DC magnetization M and the electrical resistivity. The shape of the $M(H)$ -curves is typical for type-I superconductors. The obtained phase diagram $H_c(T)$ agrees well with the literature data [6]. T_c of our sample (3.415 K) matches the tabulated value of 3.4145 K [19], and $RRR = 540$. Correspondingly, $\ell \approx 11 \mu\text{m}$ is much larger than ξ_0 . Therefore, our sample is a type-I superconductor in the pure limit.

PNR experiments were performed both on the REMUR reflectometer [20] at the Joint Institute for Nuclear Research (Dubna) and on the CRISP instrument [21] at ISIS (Oxford). Both sets of measurements confirm that splitting of the $R^+(Q)$ and $R^-(Q)$ curves is achievable for our sample. The ISIS data, which are the most detailed, allow a quantitative analysis to which we now turn.

CRISP operates with a spin-polarized polychromatic pulsed neutron beam. The angle of incidence and the instrumental resolution $\Delta Q/Q$ were set to 0.24 degrees and 3%, respectively.

The reflectivity in the Meissner state was measured at $T = 1.8 \text{ K}$ and at magnetic fields of 77, 140, 166, and 194 Oe ($H_c(1.8 \text{ K}) = 205 \text{ Oe}$). The obtained data sets are shown in Fig. 2. The $R(Q)$ -dependencies exhibit a hill caused by the total reflection from the substrate. The splitting between R^+ and R^- is clearly visible near Q_c ; different magnitudes of the error bars are due to different times of exposure. The data obtained at 77 and 166 Oe have the smallest statistical error and will be used for further discussion.

The data for the reflectivity in the normal state are shown in Fig. 3. Solid curves are simulations, in which the sample was represented by a pure In film on a SiO_2 substrate. In the simulations the angular beam resolution was allowed to vary due to the unknown uncertainties of the instrumental resolution and of the geometrical factor (as only part of the beam covers the sample).

The simulation curve near Q_c is mostly controlled by the resolution (see also [16]). The next segment, down to the foothill, is determined by the roughness of the sample surface. The location of the ascending part ($0.011 < Q(\text{\AA}^{-1}) < 0.014$) is governed by the film thickness. The curve segment following the hill is determined by the substrate scattering properties. No attempts were made to achieve a better fit for that segment, because there the spin asymmetry is indistinguishable from zero.

The best fit (Fig. 3) was obtained for the model sample with $\sigma = 14 \text{ nm}$ and $\Delta Q/Q = 2.5 \%$. Fitting the ascending part enables one to determine the film thickness *in situ*. The statistical error of the reflectivity data in this region being $\pm 5\%$, the thickness was found to be $2400 \pm 30 \text{ nm}$, in agreement with the nominal thickness of $2.5 \mu\text{m}$. These parameters were further used for simulating the spin asymmetry. Attempts to introduce an indium

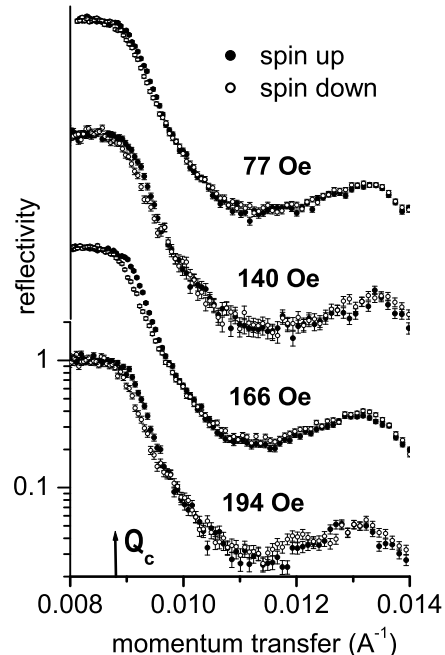


FIG. 2: Reflectivity of polarized neutrons measured in the Meissner state. Q_c is the momentum transfer for total neutron reflection from the outer surface. The scale is shown for the data at $H = 194 \text{ Oe}$; the other data have been shifted for clarity.

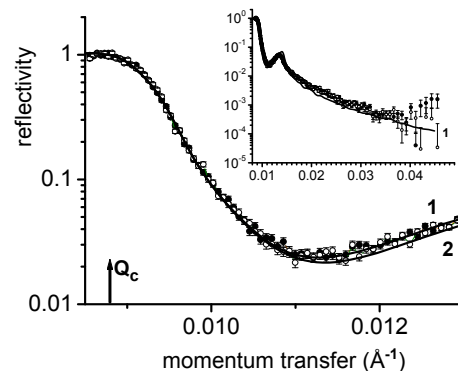


FIG. 3: Neutron reflectivity at $T = 4.6 \text{ K}$. Curves 1 and 2 are simulations for a film thickness of 2.40 and $2.50 \mu\text{m}$, respectively. The inset shows the data for the full range of Q -values.

oxide layer on top of the sample yielded no reasonable fit for any appreciable thickness ($> 1 \text{ nm}$) of the oxide layer. This is consistent with our expectation that the indium oxide layer does not affect the neutron reflectivity.

For our simulations of the reflectivity in the Meissner state, the magnetic field profiles shown in Fig. 1 were assumed on both sides of the sample. The spin asymmetry data for fields 77 Oe and 166 Oe, along with simulations

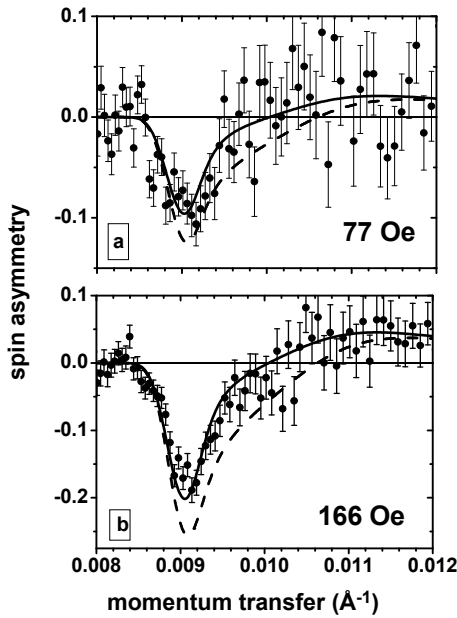


FIG. 4: Spin asymmetry at $T = 1.8$ K and $H = 77$ Oe (a) and 166 Oe (b). The curves are simulations performed within the local (dashed line) and nonlocal (solid line) approaches.

for the local and nonlocal field distributions, are shown in Fig. 4.

For field 77 Oe (Fig. 4a), the results of the “nonlocal” simulation fit the experimental data somewhat better, but no clear discrimination between the local and nonlo-

cal approaches is possible due to insufficient accuracy of the data at this field. A significantly clearer distinction is apparent for field 166 Oe due to the larger amplitude of $s(Q)$. As can be seen from Fig. 4b, the quality of the fits, with $B(z)$ calculated in the local and nonlocal approaches, is different. The nonlocal simulation fits the experimental data definitely better. It is worth stressing that *no adjustable parameters* have been used for the simulations of spin asymmetry.

In conclusion, nonlocal electrodynamics effects are measurable in extreme type-I superconductors. State-of-the-art PNR measurements performed on low- κ superconductor In, combined with simulation, unambiguously support the nonlocal theory and at the same time demonstrate consistency with the literature data for $\lambda_L(0)$ and ξ_0 . Consequently, evidence has been gathered for the nonmonotonic decay and sign reversal of the penetrating magnetic field predicted by the nonlocal electrodynamics approach.

We thank A. Volodin for AFM, S. Vandezande for electrical conductivity, and A.P. Kobzev for Rutherford backscattering measurements. This research has been supported by the KULeuven Research Council (F/05/049, GOA/2004/02), project G.0237.05 of FWO-Vlaanderen, IUAP P5/1, the European Commission 6th Framework Programme through Key Action: Strengthening the European Research Area, Research Infrastructures (Contract HII3-CT-2003-505925), Russian State contract 2007-3-1.3-07-01, INTAS grant 03-51-6426 and RFBR project 06-02-16221.

-
- [1] A.B. Pippard, Proc. R. Soc. (London) A **216**, 547 (1953). For an excellent historical account of nonlocality, see A.B. Pippard, IEEE Trans. Magnetics **MAG-23**, 371 (1987).
 - [2] M. Tinkham, *Introduction to Superconductivity* (McGraw-Hill, New York, 1996).
 - [3] J. Halbritter, Z. Physik **243**, 201 (1971).
 - [4] P. Valko, M.R. Gomes, and T.A. Girard, Phys. Rev. B **75**, 140504(R), 2007; K.S. Wood and D. Van Vechten, Nucl. Instr. Meth. A **314**, 86 (1992); I.N. Khlyustikov and A.I. Buzdin, Advances in Physics **36**, 271 (1987).
 - [5] K.E. Drangeid and R. Sommerhalder, Phys. Rev. Lett. **8**, 467 (1962).
 - [6] D.K. Finnemore and D.E. Mapother, Phys. Rev. **140**, A507 (1965).
 - [7] *X-Ray and Neutron Reflectivity: Principles and Applications*, edited by J. Daillant and A. Gibaud (Springer, Berlin, 1999).
 - [8] E. Morenzoni, F. Kottmann, D. Maden, B. Matthias, M. Meyberg, Th. Prokscha, Th. Wutzke, and U. Zimmermann, Phys. Rev. Lett. **72**, 2793 (1994).
 - [9] A. Suter, E. Morenzoni, N. Garifanov, R. Khasanov, E. Kirk, H. Luetkens, T. Prokscha, and M. Horisberger, Phys. Rev. B **72**, 024506 (2005); A. Suter, E. Morenzoni, R. Khasanov, H. Luetkens, T. Prokscha, and N. Garifanov, Phys. Rev. Lett. **92**, 087001 (2004).
 - [10] D.K. Finnemore, T.F. Stromberg, and C.A. Swenson, Phys. Rev. **149**, 231 (1966).
 - [11] G.P. Felcher, R.T. Kampwirth, K.E. Gray, and R. Felici, Phys. Rev. Lett. **52**, 1539 (1984).
 - [12] H. Zhang, J.W. Lynn, C.F. Majkrzak, S.K. Satija, J.H. Kang, and X.D. Wu, Phys. Rev. B **52**, 10395 (1995).
 - [13] R. Felici, J. Penfold, R.C. Ward, E. Olsi, and C. Maccotta, Nature **329**, 523, (1987).
 - [14] A. Mansour, R.O. Hilleke, G.P. Felcher R.B. Laibowitz, P. Chaudhari, and S.S.P. Parkin, Physica B **156-157**, 867 (1989).
 - [15] V. Lauter-Pasyuk, H.J. Lauter, V.L. Aksenov, E.I. Kornilov, A.V. Petrenko, and P. Leiderer, Physica B **248**, 166 (1998).
 - [16] K.E. Gray, G.P. Felcher, R.T. Kampwirth, and R. Hilleke, Phys. Rev. B **42**, 3971 (1990).
 - [17] M.P. Nutley, A.T. Boothroyd, C.R. Staddon, D.McK. Paul, and J. Penfold, Phys. Rev. B **49**, 15789 (1994).
 - [18] K. Temst, M.J. Van Bael, and H. Fritzsche, Appl. Phys. Lett. **79**, 991 (2001).
 - [19] *Handbook of Physical Quantities*, edited by I.S. Grigoriev and E.Z. Meilikhov (CRC, New York, 1997).
 - [20] V.L. Aksenov, K.N. Jernikov, S.V. Kozhevnikov, H. Lauter, V. Lauter-Pasyuk, Yu. V. Nikitenko, and A.V. Petrenko, [www.jinr.ru/publish/Preprints/2004/047\(D13-2004-47\)e.pdf](http://www.jinr.ru/publish/Preprints/2004/047(D13-2004-47)e.pdf).
 - [21] D.G. Bucknall, S. Langridge, and R.M. Dalgliesh,

[www.isis.rl.ac.uk/largescale/crisp/documents/manual/
crisp_manual.htm](http://www.isis.rl.ac.uk/largescale/crisp/documents/manual/crisp_manual.htm).